X-RAY INVESTIGATION OF COLLOIDAL PARTICLE SIZE IN BENT

by

MARION JOHN CALDWELL

B. S., Kansas State College
of Agriculture and Applied Science, 1931

A THESIS

submitted in partial fulfillment of the

requirements for the degree of

MASTER OF SCIENCE

KANSAS STATE COLLEGE
OF AGRICULTURE AND APPLIED SCIENCE

1933

TABLE OF CONTENTS

INTRODUCTION

In an effort to determine significant factors relating to the shrinkage losses and the keeping quality of beef, the Animal Husbandry and the Chemistry Departments of the Kansas State College have, over a period of several years, run extensive tests on the meat of cattle of definitely controlled feeding regime.

Among the tests conducted may be listed:

(1) Toughness, or shear, of fresh and ripened samples.

(2) Electrical Resistance.

(3) Percentage of total water lost in storage.

(4) Surface Distribution of Shrinkage loss.

(5) Mineral Analysis. (Sodium, Calcium, etc.)

(6) Collagen and Elastin.

(7) Keeping Characteristics.

(8) Turbidity of aqueous extract.

(9) Palatability tests.

(10) Size of Colloidal Particles.

It is with the last mentioned phase that this work is concerned, the measurement of the size of the colloidal particles of the meat. It was with the hope of correlating this factor with the other properties of the beef that these measurements were undertaken.

The term "Colloidal Particles of the Beef" is somewhat vague. The meaning of that term as here employed may better be understood by analogy to a lump of sugar. Clearly, the lump of sugar is not a crystal. But if it be more closely examined it will be found to consist of small crystals closely matted together. It is the small individual crystal of sugar that corresponds to the "Colloidal Particle" of the beef. It is the average size of these small crystals, which together make up the whole, that may be likened to the "particle size" here to be measured. Colloidal particles are, as a rule, of a magnitude of 10^{-7} to 10^{-6} centimeters, while the wave length of ordinary light is some ten times as great. For this reason visual or microscopic methods of measurement are of no avail. Other methods, direct or indirect, must be employed.

Roentgen rays (X-rays), since they are akin to light except for a wave length magnitude of 10^{-8} centimeters, are capable of being diffracted by particles of colloidal size. These rays because of their penetrating power may be used to study materials in their original state of aggregation, i.e. without extensive preparation of the sample. The method of measurement by diffraction is a more direct and generally applicable method than those based upon adsorption, covering power, or other properties characteristic

of the material being studied. In addition, the X-ray method gives information as to the crystalline structure of the sample that no other method can give. It is for these reasons that the X-ray diffraction method is here employed.

HISTORICAL

X-Ray in General

Roentgen, in 1895, while working with cathode ray tubes, discovered the rays which were later to bear his name. These rays, produced wherever cathode rays are stopped by matter, were invisible and possessed many properties common to ultra-violet light. They excited photo-electric effects, caused fluorescence in many materials, and affected photographic plates. In addition, these new rays were extremely penetrating, transversing the human body and even steel. Attempts to focus the rays by refraction, to reflect them from mirror surfaces, or to obtain interferences from diffraction gratings proved fruitless.

Since that time it has been definitely proved that Roentgen rays are very short electromagnetic waves, as are visible light waves, and that the differences exhibited by them are quantitative and not qualitative. The limits of wave length of X-rays are somewhat arbitrary. Clark (3)

gives these limits as from 0.06 to 1019.00 x 10^{-8} centimeters.

X-Rays in Crystal Study

The year 1912 marks a new era in the understanding of the solid state of matter. In that year, Laue at the University of Munich reasoning from crystallographic facts suggested that if crystals were, in reality, regularly marshalled molecular or atomic groups, and if the new rays were electromagnetic waves, then (since the magnitudes of the rays and crystal lattice were thought to be the same) interference effects should be evident when the rays impinge on a crystal surface. This reasoning proved sound; and as a result both crystallography and Roentgenology have been placed on a firm foundation. With the facts of diffraction known, the study of the inner structure of crystals, and indeed even of the molecule, was begun. Today the microstructure of many crystals, dimensions and configurations of certain molecules, and the characteristics of pure liquids and solutions are to be found in the literature.

X-Ray for Particle Size Measurement

A few years later it was pointed out by Debye and Scherrer that the size of fine particles might be measured

by the use of X-rays. It was known that a visible light of monochromatic character appears as a single line, sharp and distinct, in a spectroscope using a long diffraction grating; while the same spectral line becomes wider and blurred as the grating is made effectively shorter by covering part of its length with an opaque shield. The ability of a grating, prism or lens system to give sharp interferences (clear cut lines or images) is known in optical parlance as the resolving power of the system. In each case the resolving power is a direct linear function of some dimension of the optical equipment concerned. In a diffraction grating the ability to give sharp spectral lines is a direct function of the total length of the ruled surface. If, then, the width of a known spectral line from a given grating is measured the length of the grating can be calculated.

Identical relations exist in the X-ray ring patterns. The Debye-Scherrer ring is but a composite of the interferences produced by myriads of extremely small colloidal particles of the sample, each particle of which is acting as a separate and individual diffraction grating in the X-ray beam. It is the width of this ring which bears a quantitative relation to the size of the particles causing it, and by virtue of this relation the measurement of the colloidal particles becomes possible.

Debye and Scherrer were the first to derive the quantitative relation referred to above. Selyakov, Bragg and others have since derived similar equations for the same purpose. These various equations differ from each other somewhat in make-up, but check the original Debye-Scherrer derivation within a few percent in the colloidal range. The particles in gold sols thus measured are shown by Clark (3) to have dimensions of from twenty-one to one hundred thirty Angstrom Units (10^{-8} centimeters).

THEORETICAL

Fundamental Equations

Laue's original work relating to X-ray interferences from crystals involved the conception of interferences from a three dimensional space lattice. The reasoning, while rigorously exact, involves mathematical difficulties which are very conveniently avoided by the method of Bragg as given by Crowther (7), wherein the crystal is considered as a reflection grating. By this concept may be derived the fundamental law of X-ray diffraction, $n\lambda = 2\ d\ \mathrm{Sin}\ \theta$.

This fundamental formula, almost identical to the diffraction grating relation for visible light, may be derived in a number of ways. The following, from Crowther, is among the best.

The lines pp, qq, and rr (Text Fig. 1.) represent three parallel planes of the crystal, successive planes being d distance apart. P, P', P'' are parallel X-rays impinging on the crystal at an angle, θ. At each surface (lines in the Figure) very weak reflections of the rays will take place at an angle equal to the angle of incidence; but these various reflections will individually be too weak to have appreciable effect. However, where reflections from the series of planes reinforce each other a relatively intense beam will result. This reinforcement will occur where the difference in path of the rays from successive planes is an exact multiple of the wave length, i.e. all reflections in phase.

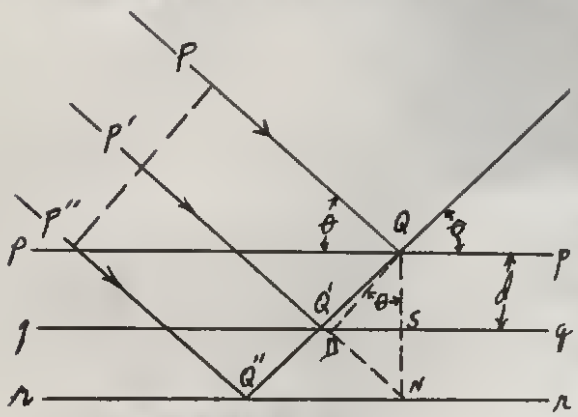

Text Fig. 1.

Drop Q'N perpendicularly to qq; and draw QD perpendicular to P'N. Now since QN is perpendicular to qq and angle SQ'Q and angle SQ'N are equal, Q'N equals Q'Q. Now the difference in path between ray P and P' is :

$$P'Q' + Q'Q - PQ = P'Q' + Q'N - P'D$$

$$= DN$$

$$= QN \sin \theta$$

$$= 2\,d\,\sin\theta$$

But, for reinforcement, this difference in path must be equal to an integral number of wave-lengths, n, hence the equation becomes,

$$n\lambda = 2\,d\,\sin\theta\ .$$

This equation is to be compared with the general diffraction grating equation as given by Baly (1):

$$n\lambda = b\,(\sin i + \sin\theta)$$

In X-ray work since the angle of incidence must always be equal to the angle of diffraction, the i and θ of the general equation are equal, and the equation reduces to

$$n\lambda = 2\,d\,\sin\theta\ .$$

This derivation reveals that reflection from a crystal will occur only when the crystal is set at such an angle to the impinging ray that the above relation is satisfied, including the fact that the angle of deviation of the primary beam is twice the angle of diffraction, θ.

Resolving Power

By the above equation it is seen that complete reinforcement will take place only in the direction which makes an angle θ with the crystal. Obviously then, at some angle $\theta \pm d\theta$ interference will occur and the intensity will be reduced to zero. What factors influence the value of the angle $2\,d\theta$, within which band there is some resultant

radiation? For reasons which will be given presently the line width will be considered not the distance from zero to zero intensity of radiation, but rather from one half of the maximum intensity on one side to the corresponding point on the other side of the maximum.

The phenomena of interference must be considered in the light of Huyghen's principle. Each particle in the crystal is excited by the primary X-ray and sends out secondary wavelets of the same frequency as the exciting wave and in all directions. Under certain conditions (as indicated by the fundamental equation) these wavelets may all be in phase, producing an intense beam in that direction. At any other angle, regardless of how close to the angle of reinforcement, the successive waves will be slightly out of phase. If, then, the diffracting medium is thick enough, each wavelet will find another exactly one hundred eighty degrees out of phase with it, and interference will be complete. If, on the other hand, the diffracting system is somewhat smaller, some of the wavelets will be unable to find their oppositely phased counterpart, and some radiation will persist. From this reasoning it follows that the sharpness of the interference is a function of the thickness of the regularly ordered system creating the interference, the crystal grating.

Particle Size Equations

Merely the above concept of the mechanism of interference would indicate that a sharp diffraction ring from a mass of fine particles would mean relatively large size crystal fragments, while a wide, blurred ring would indicate a small number of planes involved in the interference reactions. Debye and Scherrer, after whom the powder patterns are named, were the first to devise a quantitative relationship between the angular breadth of the ring and the particle size. Their formula is given as follows:

$$B_{(Scherrer)} = 8\sqrt{\frac{\ln 2}{\pi}} \cdot \frac{\lambda}{D} \cdot \frac{1}{\cos\frac{\alpha}{2}} + b$$

where B is the angular breadth of the ring in radians, λ is the wave-length of the monochromatic X-ray used, D is the diameter of the colloidal particle or crystal fragment in Angstrom Units, α the angle of deviation of the primary ray, and b is a constant depending on the particular equipment used. The writer has not seen the derivation of this formula, but it appears similar to the "Breadth of Spectrum Line" formula as given by Baly (1).

$$\text{Breadth of Line}_{(\text{wave-lengths})} = \frac{1}{\pi} \cdot \sqrt{\frac{\ln 2}{\pi}} \cdot \frac{\lambda^2}{V}$$

Polyakov and Bragg give similar relations:

$$B_{(Selyakov)} = \frac{2\sqrt{3 \ln 2}}{\pi} \cdot \frac{\lambda}{D} \cdot \frac{1}{\cos \frac{x}{2}} + b$$

$$B_{(Bragg)} = 0.89 \frac{\lambda}{D} \cdot \frac{1}{\cos \frac{x}{2}} + b$$

where all terms have the same significance as in the Debye equation. These formulae check within a few percent in the colloidal range.

It was believed these formulae were too involved to handle rapidly in the present work, hence the writer undertook to develop an equation more applicable to his problem. The following formula is not new. It is but a revision of the standard resolving power formula for diffraction gratings, adapted to the Debye-Scherrer X-ray ring patterns.

It has been shown that the diffraction grating formula $n\lambda = d(\sin i + \sin \theta)$ reduces when applied to X-ray work (where the angles of incidence and diffraction are equal) to $n\lambda = 2d \sin \theta$, the fundamental X-ray diffraction relation. Using the former equation together with the resolving power concept of Lord Rayleigh, Baly (1) develops the resolving power formula for the diffraction grating:

$$r = \frac{f}{\lambda} (\sin i + \sin \theta)$$

where r is the resolving power of the grating, f the total effective length of the ruled portion, λ the wave length concerned, and i and θ of their usual significance. Now,

by definition, $r = \frac{\lambda}{d\lambda}$

and in X-ray phenomena, angle i = angle θ, hence,

$$\frac{\lambda}{d\lambda} = \frac{f}{\lambda} \cdot 2 \sin\theta$$

$$f = \frac{\lambda^2}{d\lambda} \cdot \frac{1}{2 \sin\theta} .$$

In this equation if the wave length is in Angstrom Units, f is the particle thickness in the same units. The angle θ is the angle of diffraction (one half angle of total deviation). The line or ring breadth is in terms of $d\lambda$, that is, the difference in wave length between two successive waves which would just be "resolved" or shown as separate lines, using the sample being measured as the diffracting medium in an X-ray spectrograph.

This minimum change in wave length necessary for the appearance of two separate lines will evidently be very close to the difference between two waves that would center at the two points of one-half maximum intensity of the ring. This will be made more apparent by the adjoining diagram.

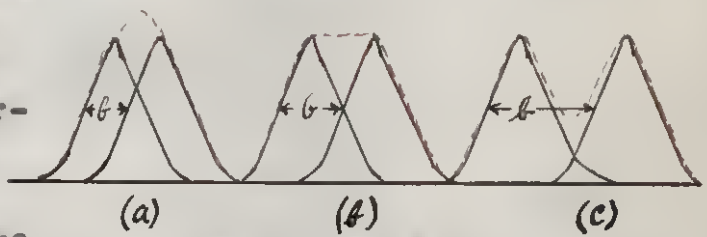

Text Fig. 2.

It may be seen from the diagrams that in case the two waves are closer together than the distances between points of half-maximum intensity, the resultant wave form cannot be

distinguished from a single intermediate wave (a). In case the distance between the two waves is just equal to the distance between the half-maximum intensities, the limiting condition arises (b). When the separation of the waves is greater than the half-maximum distance the existence of the two waves becomes evident. The exact shape of each wave will have some bearing on the result, but by this rudimentary explanation the reason behind the apparently arbitrary measurements of the "half-breadth" of the band becomes understandable.

By measuring the radius of the Debye-Scherrer ring the space-lattice constant (d in the formula) may be determined. Then knowing the d, and the distances from the center to the points of half-intensity, the $\frac{d\lambda}{}$ may be determined by re-application of the law, $n\lambda = 2d \sin\theta$. A more convenient method of determining the $\frac{d\lambda}{}$ is to make a graph of λ plotted against the distance on the film from the undeviated beam. Then by direct reading on the graph of the λ's corresponding to the two half-maximum distances from the center, the $\frac{d\lambda}{}$ is determined.

It has been experimentally found that with all meats studied the radius of the ring produced is a constant, with in the limits of experimental error (17mm. radius at 60 mm. from sample). Since this unexpected condition exists, and

since the same radiation was used throughout the work, the above formula may be very conveniently reduced from

$$f = \frac{\lambda^2}{2 \sin \theta} \cdot \frac{1}{d\lambda}$$

to

$$f = \frac{K}{d\lambda}$$

Hence, for any particular material being studied (meat), the particle size may be determined simply by the use of the one constant (7.33 in the case of meat) and the "$\frac{\lambda}{}$ vs. displacement" curve.

This method of particle measurement differs from the other formulas by the use of the sine rather than the cosine function, and by the use of ring breadth in terms of $\frac{d\lambda}{}$ rather than radian measure. It has been compared with the Debye-Scherrer and the Bragg formulas in the particle size range here encountered, and found to check them as well as they check each other.

Measurement of Ring Breadth

With the Debye-Scherrer ring patterns at hand and the particle size equations a matter of choice, there remains a very important phase of the work yet to be done--the actual measurement of the breadth of the band at half-max-

imum intensity. As a first step in this measurement, the information contained on the X-ray film must be converted into a curve for study. This curve must show the relative intensity of the radiation striking the film at each point along any chosen radius. For this purpose a micro-photometer using a photo-electric cell was employed (See Fig.2). Very obviously, from the experimental curve thus obtained (Fig.3) it appears that the ring is not alone on the film, but is superimposed on a more intense background of some other origin. The ring breadth cannot be measured until the nature of the background is fully understood.

Close scrutiny of the complete assembly used when the picture was taken (Fig.1) reveals other possible sources of radiation. First, the intense X-ray beam, of which only a very small part is diffracted, penetrates the meat and impinges on a small lead cup on the film holder. The ray is very effectively stopped by the lead, and does not record on the film. The beam in its passage from the meat sample to the lead cup, however, transverses five centimeters of air. The air molecules struck by this powerful beam are excited, and each molecule in the path of the primary ray becomes the center for the emission of secondary radiation. The secondary rays reach the film and leave their record. Likewise, the individual molecules of the meat sample also

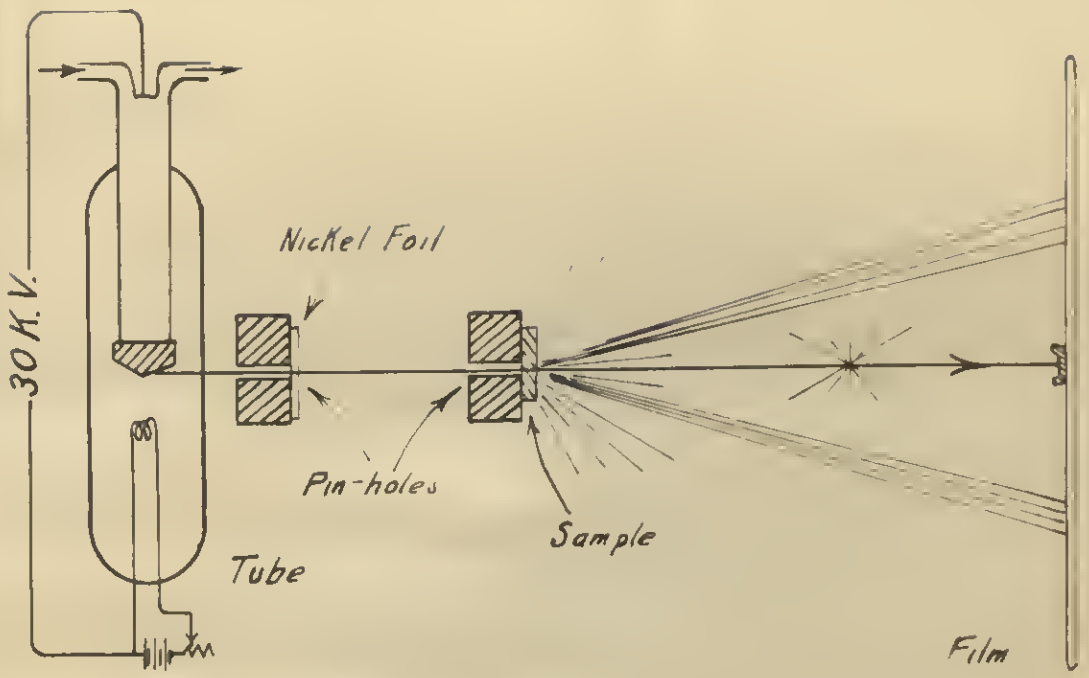

Fig. 1. Diffraction Assembly

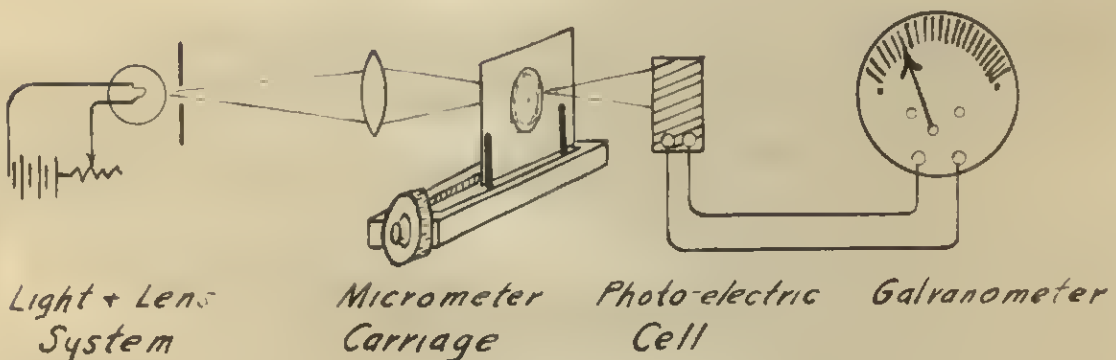

Fig. 2. Micro-Photometer

Plate II

Fig. 3. Showing Original Meat Curve to Absolute Scale

Sample Number 149

become secondary radiators, quite apart and independent of the directed radiation of the diffracted rays. The rays there sent out also find their mark in the photographic film. On the one film then, presumably containing only the diffraction ring of the sample being studied, are found the cumulative effects of at least these three separate and distinct sources of radiation. Can they be separated and studied individually?

Air-Scattering Equation. To arrive at the effect of air alone, a photograph may be made using no sample over the pinhole. This procedure gives a definite pattern, which when run on the micro-photometer shows graphically the effect of the air. But the absolute magnitude of this "air curve" will depend on the rate at which the tube was operating, the film used, the developing solutions and time, the time of the run and the intensity of the light used in the micro-photometer. The exact shape of this air curve may better be derived by the methods of calculus.

In Text Figure 3 the diffraction assembly is shown in skeleton form. The X-ray beam limited by the pinhole system, strikes the meat sample and thence proceeds through the air to its stopping place in the lead cup on the film. Now, the intensity of the air-scattered ray at any point on the film, x , will be the summation of the intensity of

all the waves reaching point x from the air molecules along the line of propagation of the primary ray, i.e. the Y-axis.

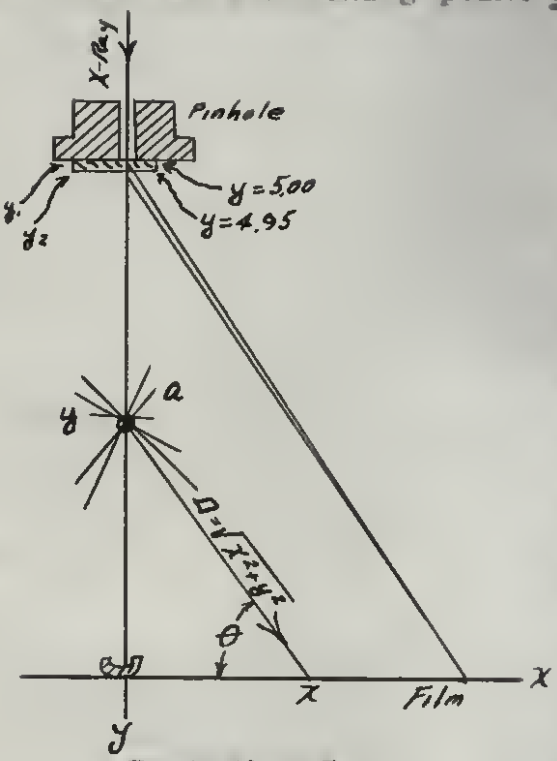

Text Fig. 3.

Also, the intensity at the film of radiation from any molecule of air will be directly proportional to the sine of the angle of incidence, inversely proportional to the distance squared, and directly proportional to a radiation constant a of the molecule involved. Hence,

$$I_x = \sum_0^{y_1} \frac{a}{D^2} \cdot \sin\theta$$

$$I_x = \sum_0^{y_1} \frac{a}{\left(\sqrt{X^2+Y^2}\right)^2} \cdot \frac{Y}{\sqrt{X^2+Y^2}}$$

$$I_x = \int_0^{y_1} \frac{a}{\left(\sqrt{X^2+Y^2}\right)^3}\, dY$$

$$I_x = -a\left[\left(X^2+Y^2\right)^{-\frac{1}{2}}\right]_0^{y_1}$$

Setting the limits of integration as they are in practice at 0.00 and 4.95 centimeters, and evaluating:

$$I_x = \frac{a}{X} - \frac{a}{\sqrt{24.5+X^2}}$$

This last equation gives the intensity of blackening on the X-ray film at any distance x from the undeviated central beam which may be traced to the scattering effect of the air. The evaluation of the constant a will depend upon the particular conditions under which the photograph was taken and the units chosen, but (as will be seen later) will be considered only relative to the other values to be determined.

Of primary interest is the check the above equation affords for both the X-ray and micro-photometric technique here employed. Experimental curves obtained from the air-scattering alone when plotted to the same scale and on the same paper as the above equation agree with it completely, within narrow limits of experimental error (See fig.9).

Amorphous Heat Scattering Equation. Very similar considerations obtain in the calculation of the amorphous scattering from heat. In this case the limits of integration are from 4.95 to 5.00 centimeters, and the radiation constant will be termed "b".

$$I_{x(Heat)} = -b \left[\left(X^2 + Y^2 \right)^{-\frac{1}{2}} \right]_{4.95}^{5.00}$$

$$I_{x(Heat)} = \frac{b}{\sqrt{24.5 + X^2}} - \frac{b}{\sqrt{25.0 + X^2}}$$

This last equation gives the intensity of blackening on the X-ray film at any distance x from the undeviated central beam which may be traced to the scattering effect of the air. The evaluation of the constant a will depend upon the particular conditions under which the photograph was taken and the units chosen, but (as will be seen later) will be considered only relative to the other values to be determined.

Of primary interest is the check the above equation affords for both the X-ray and micro-photometric technique here employed. Experimental curves obtained from the air-scattering alone when plotted to the same scale and on the same paper as the above equation agree with it completely, within narrow limits of experimental error (See Fig.9).

Amorphous Meat Scattering Equation. Very similar considerations obtain in the calculation of the amorphous scattering from meat. In this case the limits of integration are from 4.95 to 5.00 centimeters, and the radiation constant will be termed "b".

$$I_{x(Meat)} = -b \left[\left(X^2 + Y^2 \right)^{-\frac{1}{2}} \right]_{4.95}^{5.00}$$

$$I_{x(Meat)} = \frac{b}{\sqrt{24.5 + X^2}} - \frac{b}{\sqrt{25.0 + X^2}}$$

it will be noted that in the original integration one basic assumption was that the molecule becomes a "center" of radiation, that is, it radiates with a or b intensity in all directions, upon being excited by the primary beam. This is not in reality the case (7,6). Secondary radiations are emitted in all directions from a body, but not at equal intensity in all directions. This erroneous assumption does not invalidate the relations derived in the case of the air-scattering. This is because of the fact that where the angle of scattering is far from the median, either the greater distance to the film or the smaller angle of incidence minimises the effect. With the meat-scattering this condition does not obtain, as each point receives its total radiation at a very nearly constant angle to the central beam (Text Fig.5).

The unequal radiation does become appreciable in the case of the meat, and a correction factor (Fig.4), depending on the angle to or distance from the central beam, must be applied to the calculus equation. The determination of this so-called "scattering-factor" involved the use of a circular vacuum camera designed especially to avoid all sources of radiation except that due to the meat sample alone. The complete equation for the amorphous meat scattering is:

$$I_x \left(\frac{b}{\sqrt{24.5 + x^2}} - \frac{b}{\sqrt{25.0 + x^2}} \right) \cdot S.F.$$

It will be found convenient to consider the air and amorphous meat scattering not separately but together when they are to be subtracted from the complex curves being measured. In what proportions should the two curves be added to give the true base line upon which the Debye-Scherrer ring is superimposed? The answer to this question was not found in the literature, nor was it determined by the writer. A logical assumption to make is that the radiation constants are directly proportional to the densities of the two materials:

$\frac{a}{b}$ :: Density of air ; Density of meat

This assumption was made, and has been used throughout the work. The ratio of the densities was determined, giving b a value of one thousand times a.

Since the scattering-factor of the meat is not known as a function of λ, it was thought best to combine the two curves graphically. This was done, and the resultant curve (when reduced to the proper scale) becomes the base line upon which all the particle size measurements depend. It is upon this intense background that the regularly diffracted rays from the crystal lattice of the meat are superimposed.

Effect of Heterogeneous X-Ray. Thus far the primary X-ray beam has been assumed to be a pure monochromatic

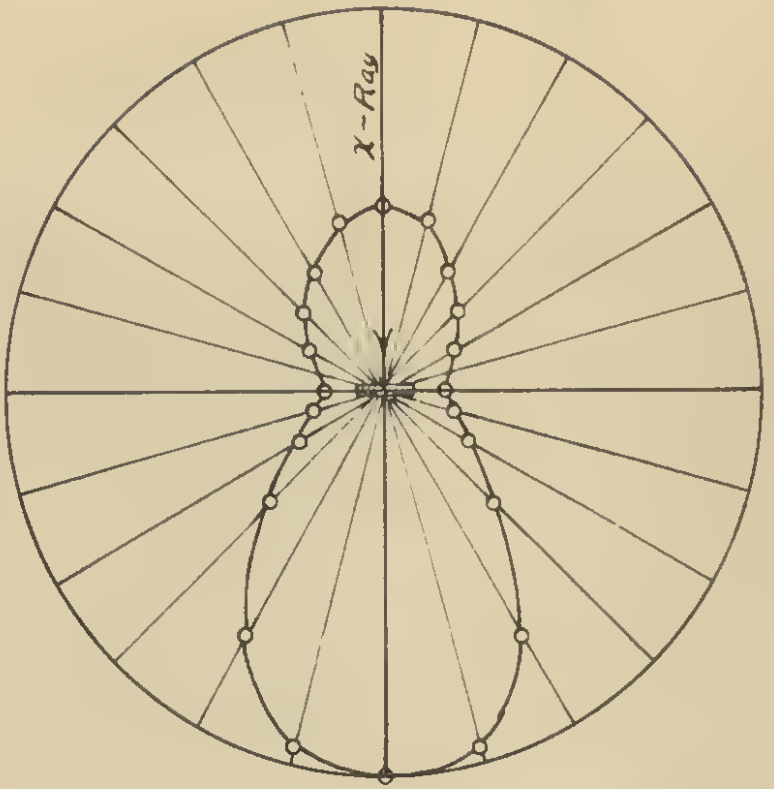

Scattering Factor
Film 5.0 Cm from Pin-hole

Cm from Center	Factor
0.0	1.00
1.0	.98
2.0	.90
3.0	.72
4.0	.50
5.0	.38

Fig. 4. Secondary Radiation from Meat

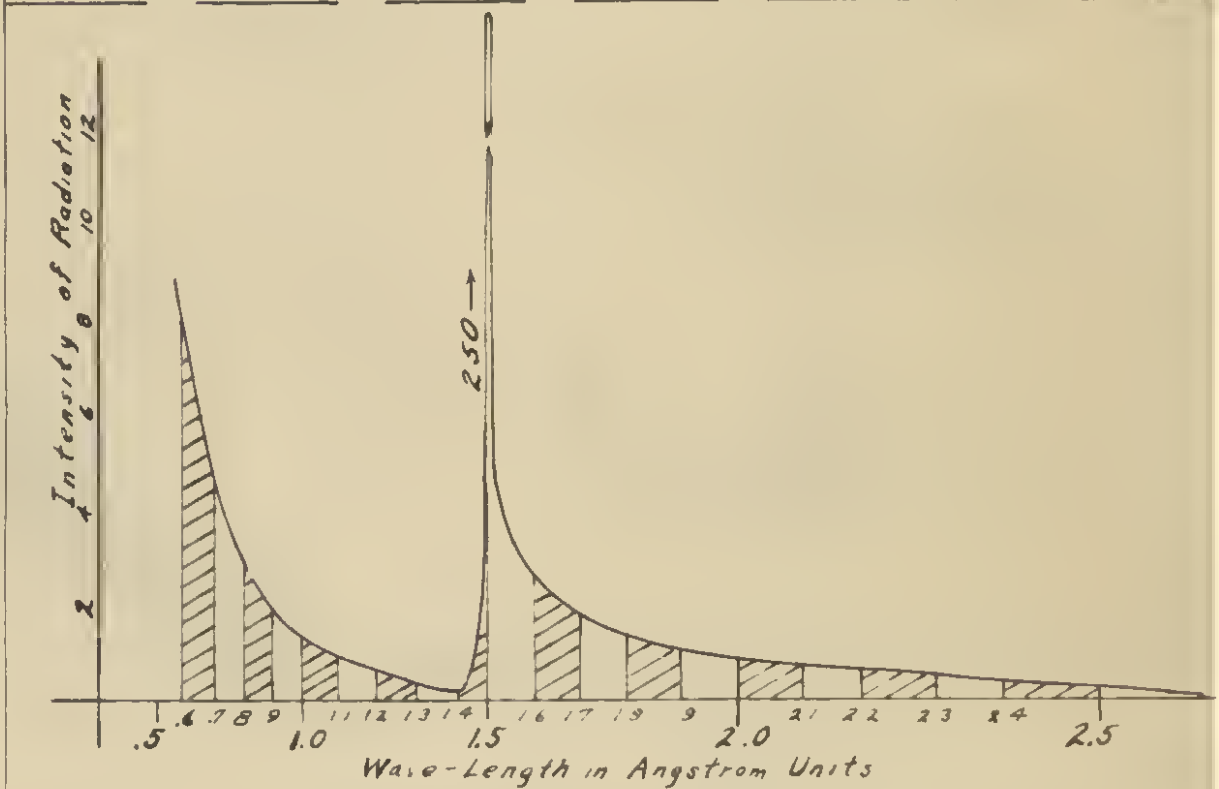

Fig. 5. Intensity Distribution of Nickel Filtered Copper Radiation – 30. K.V.

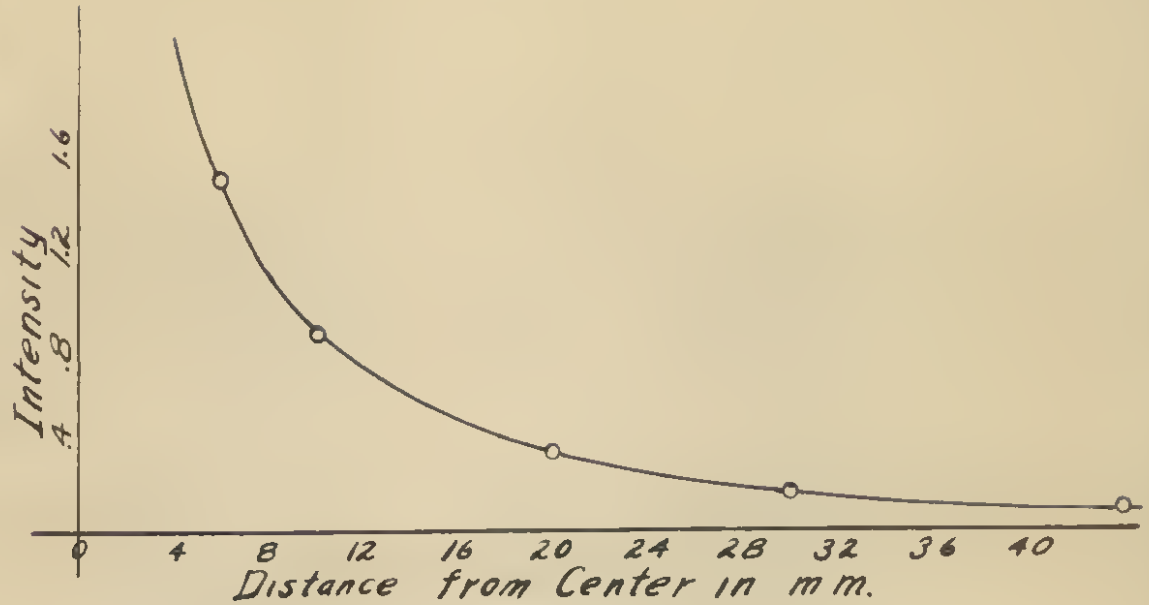

Fig.6. Air Scattering Curve

$$I_x = \frac{1}{x} - \frac{1}{\sqrt{x^2+24.5}}$$

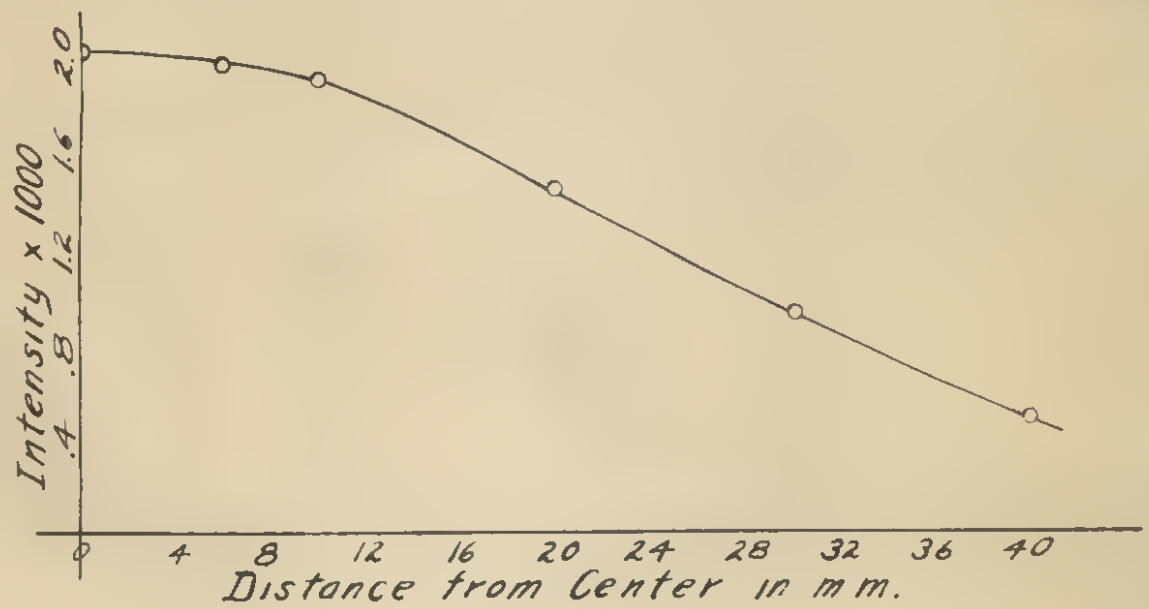

Fig. 7. Amorphous Meat Scattering

$$I_x = \left(\frac{1}{\sqrt{24.5+x^2}} - \frac{1}{\sqrt{25+x^2}}\right) \times S.F.$$

Plate V

Fig. 8. Showing Base-Line due to general scattering from Meat + Air.

Curve (A) - Air-Scattering — $I_x = \frac{1}{x} - \frac{1}{\sqrt{x^2 + 24.5}}$.

Curve (B) - Meat-Scattering — $I_x = \left(\frac{1}{\sqrt{x^2+24.5}} - \frac{1}{\sqrt{x^2+25}}\right) \times S.F. \times 1000.$

Curve (C) - (A) + (B)

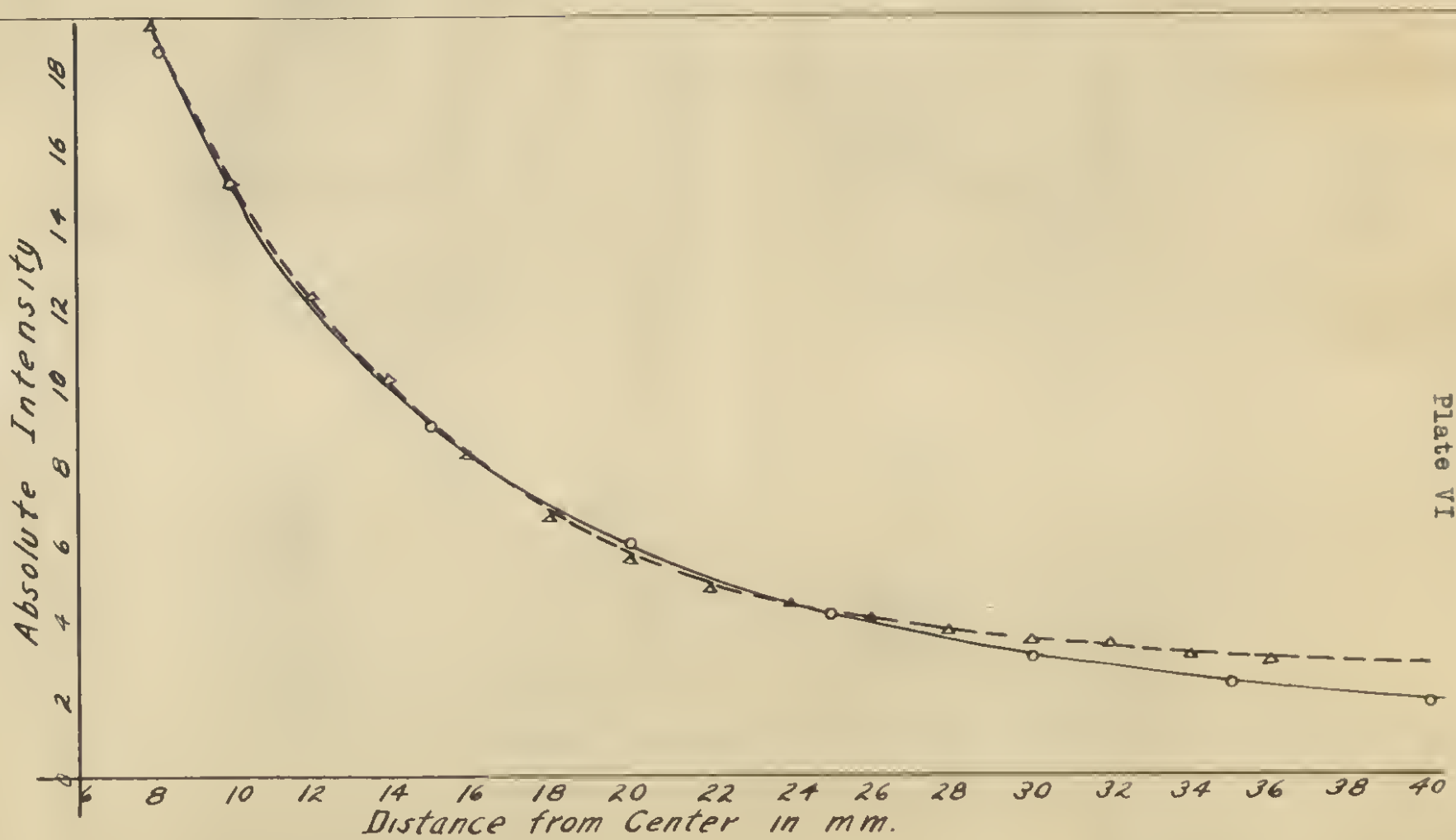

Plate VI

Fig. 9. Theoretical and Experimental Air Curve

o -- Calculated, ($I_x = \frac{1}{x} - \frac{1}{\sqrt{x^2+24.5}}$) ; Δ -- Experimental

radiation. This is, unfortunately, not the case. Despite operating the tube at optimum voltage and using carefully selected filters, the total energy of the ray is far from being concentrated in the immediate vicinity of the K_α line of copper, at 1.541 Angstrom Units. The derivation of the foregoing equation for the air and meat scattering were not concerned with the wave length of the exciting beam, and hence remain valid. But, where the radiation is directed toward the film according to the law, $n\lambda = 2\,d\,\mathrm{Sin}\theta$, the purity of the ray is of primary importance. Complete purity of the ray can only be closely approached by reflecting the primary radiation from a crystal surface, and then only at the almost prohibitive expense of intensity. This procedure was not employed, hence the heterogeneity of the ray must be taken into account in the interpretation of the resultant patterns.

By means of an oscillating sodium chloride crystal spectrograph the exact character of the radiation was determined. The total radiation was then divided into increments of finite width (increments between 1.0 and 1.1; 1.1 and 1.2; 1.2 and 1.3 Angstrom Units, etc.) and the energy represented by each increment measured (Fig.5). By assuming a definite size particle of known space-lattice, the effect of each increment on the film, both as to relative intensity and location, may be plotted. By plotting on one

graph all of the rings which would be produced by the increments, each wave-length increment considered acting independently of the others, and then by combining these into a resultant curve, the shape of the curve that may be expected using the particular X-ray beam and particle size will be obtained (Fig.10). Repetition of this procedure, assuming various particle sizes reacting with the known ray, furnishes data by which to construct a "Stripping" curve (Fig.11). By the use of this "Stripping" curve the pattern obtained using the mixed ray may be stripped or pared down to the curve corresponding to the pure K_{α} radiation. Examination of figures 10 and 11 will clarify this rather involved plan to arrive at the symmetrical curve, which would have been obtained had a true monochromatic radiation been available.

Disintegration of Complex Curve

Using the photometric graph of the Debye-Scherrer rings, the base line curve, and the "stripping" factors, it is now possible to disintegrate the original pattern, and reduce it to the pure form as demanded by all particle measuring equations. This desired form is the hypothetical curve or ring which would have been produced had the exciting X-ray been entirely homogeneous, and had the air

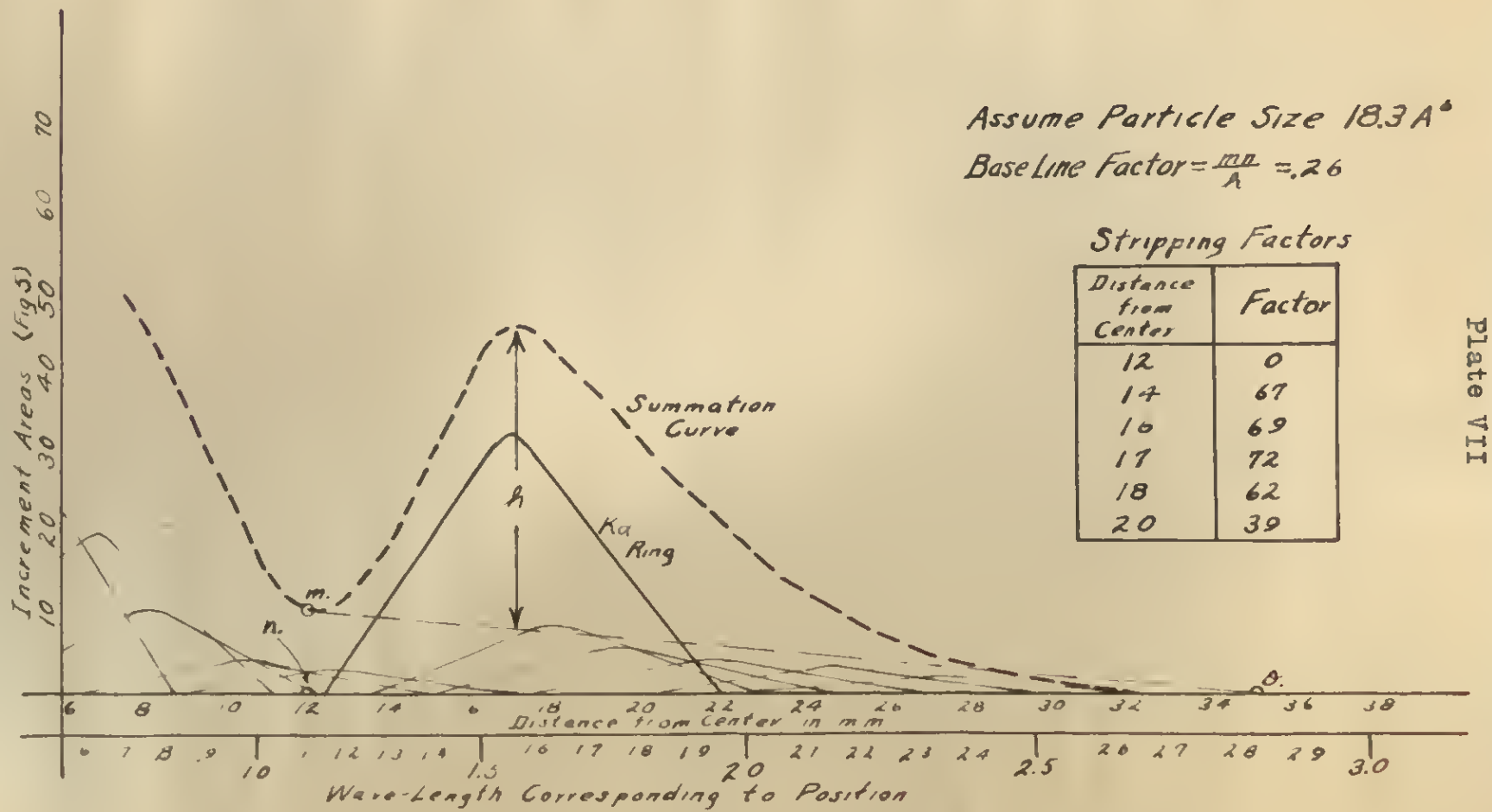

Plate VII

Fig.10. Showing Effect of Non-homogeneous Radiation

Note:- Not all increments (Fig.5) are shown.

and meat molecules produced no scattering effect. The effect of each of these causes has been determined and may now be taken from the composite, leaving the desired pattern.

Certain assumptions precede the complete unraveling of the added effects of the various sources of radiation. Free reference will here be made to Figure 12.

Assume:

(1) Intensity of radiation from meat and air molecules is proportional to their respective densities.

$\frac{a}{b}$ :: Density of air : Density of Meat.

(2) Point "c" (Fig.12) is not influenced by the Debye ring, but represents a point on the base line.

(3) Point "n" (on the curve 12.0 mm. from center) through which the base line passes is a constant proportion of "h" below "m", for any one size of crystal fragment.

(4) The curve due to the K_α radiation of copper is a definite function of the Summation curve, (Fig.10) for any one particle size.

Assumption (1) has been previously discussed and has been found to give reasonable results. Assumption (2) is based upon a study of the general shape of many meat curves (Fig.3). The point "c" (35 mm. from center of the ring) apparently falls outside of any ring effect, and hence is taken as one point on the base line. Any other

point outside the influence of the ring proper might have been selected as the point "o". A study of the summation curve construction will bear out the validity of assumption (3). Number (4) assumption also follows directly from the construction of the summation curve (Fig.10).

It will be noted that two of the above assumptions were made on the premise of a particular "particle size". This "particle size" is the dimension being measured in the work; hence, the assumptions used in the measurements are predicated by a preliminary knowledge of the final result. Such a condition results in an inability to proceed directly to the goal, and necessitates an estimation of the final result before additional progress may be made. This is exactly the procedure followed in the present work.

The size of the particle is estimated as a preliminary step in the measurement. This original "guess" then fixes the relations (3) and (4) above. Point "n" is located by reference to the stripping chart, and the base-line to the proper scale (set by the relation of points "n" and "o" through both of which it must pass) is drawn through points "n" and "o". The difference in ordinates of the original meat curve and the assumed base line is plotted immediately below the original. The "stripping" factors are applied (Fig. 11) and a third curve, this time completely

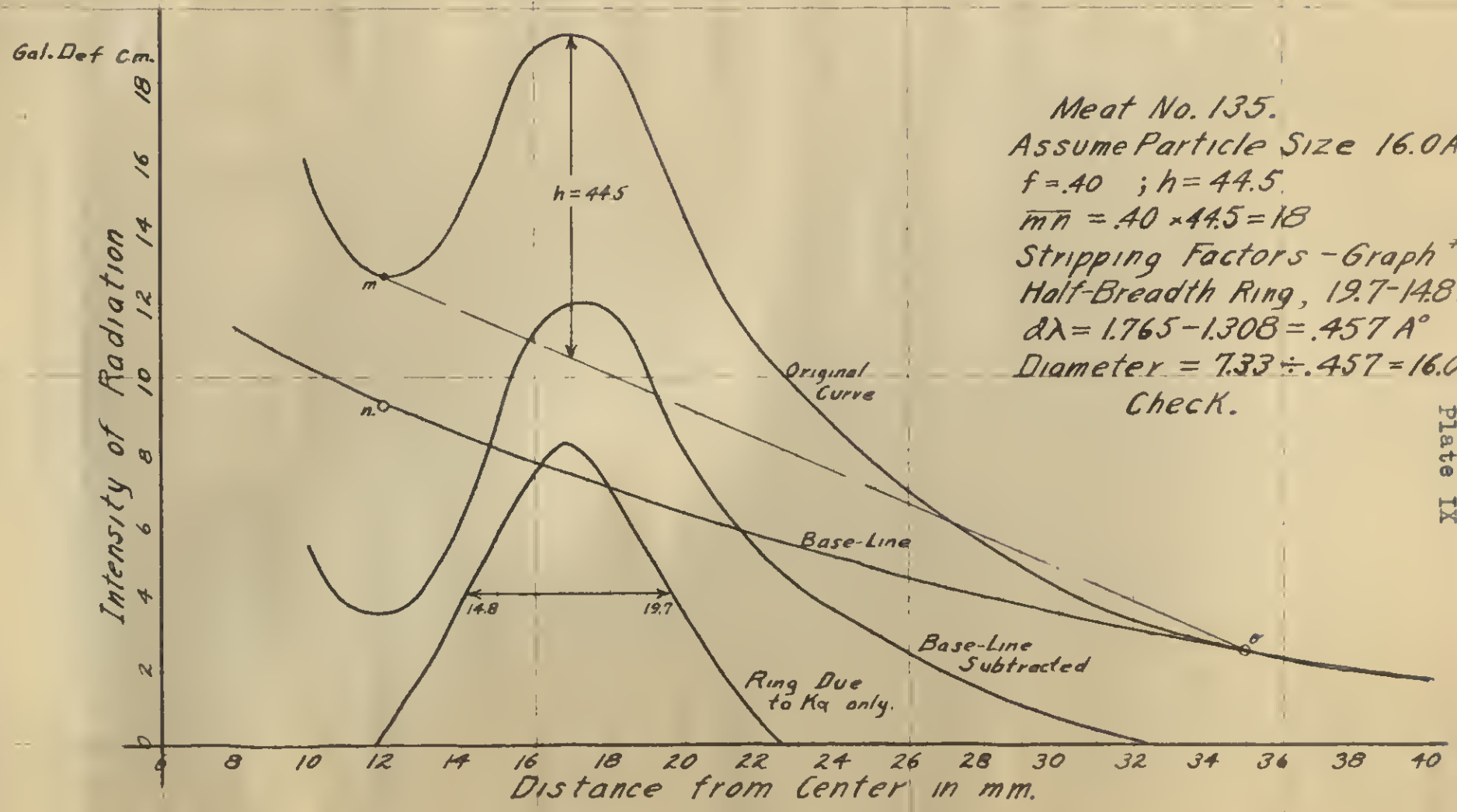

Meat No. 135.
Assume Particle Size 16.0A°
$f = .40$; $h = 44.5$
$\overline{mn} = .40 \times 44.5 = 18$
Stripping Factors - Graph #11.
Half-Breadth Ring, 19.7-14.8 m.m
$d\lambda = 1.765 - 1.308 = .457$ A°
Diameter $= 7.33 \div .457 = 16.0$ A°
Check.

Plate IX

Fig. 12. Particle Size Measurement

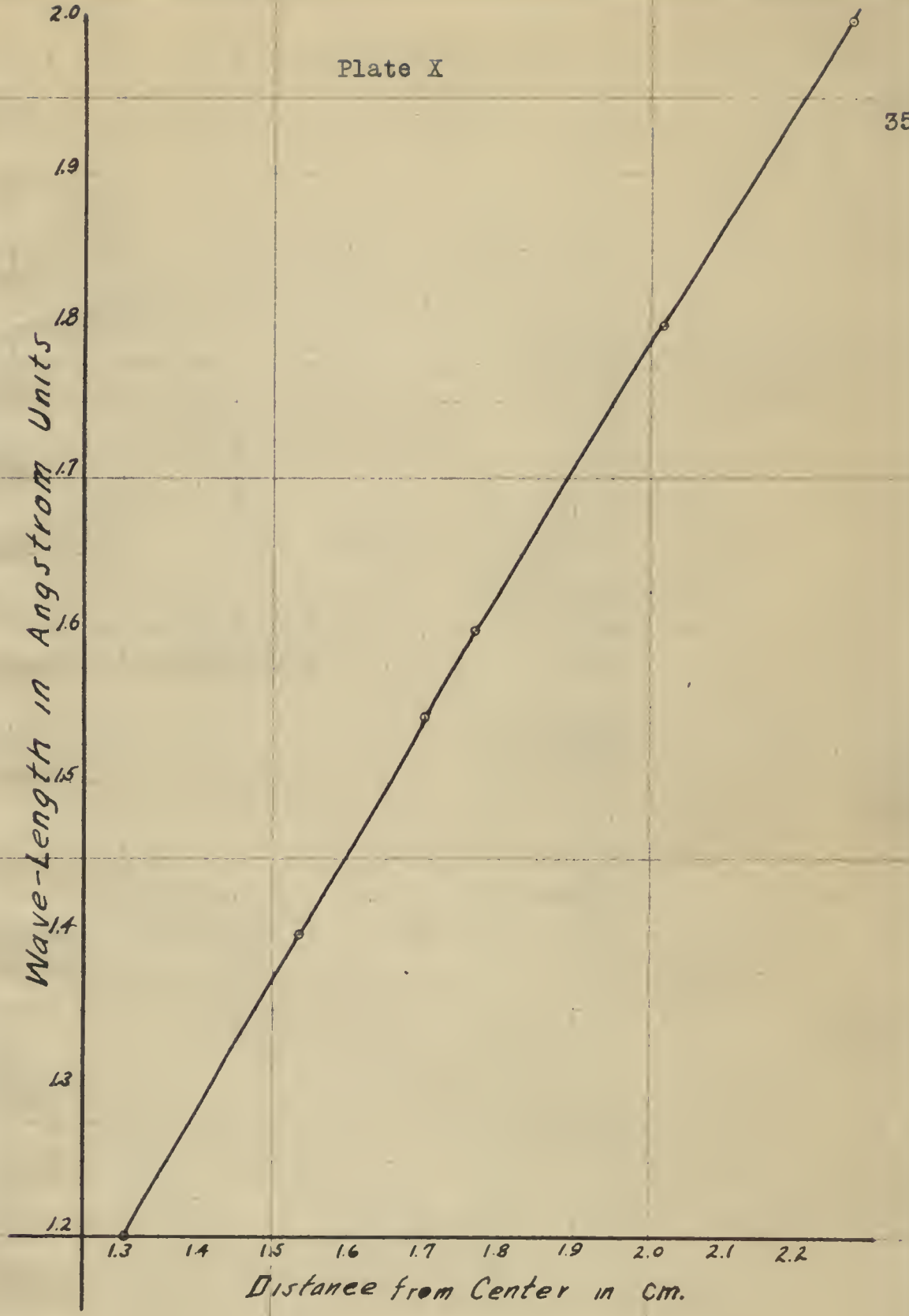

Fig. 13

Showing Relation between λ in A° and Distance from Central Beam, where $d = 4.73$ A°

freed of the base line and the effects of the heterogeneous radiation is obtained. Measurement of the half-breadth of this curve when substituted in the resolving power formula gives a "value" for the particle size. Now, if the original estimate of the particle size was accurate, the value arrived at by the above process will be the same as the estimate, and the particle size measurement will be complete. If, however, the original guess was inaccurate the arrived at "value" will not check; in which case the assumed size was in error, and the whole process must be repeated until the estimate is proved correct.

Discussion of the Method Employed

This method of solving a complex problem is of course not as direct as desirable. However, when many independent variables combine to produce a single measurable effect (the darkening of the photographic film) the separation of the effects of each factor becomes a very involved problem not always capable of any solution. The method here employed has in reality been one of synthesis rather than analysis. The separate factors were in themselves minutely analysed, and then by a reversed process built into a complex, which if the proper elements were selected and combined in the proper proportion would result in the

original Debye-Scherrer pattern.

Some very recent investigators have greatly minimized the complexity of similar problems by ingeniously carrying out the photographic operations in an atmosphere of hydrogen rather than air, and by using X-rays reflected from rock salt as a source of mono-chromatic radiation. The writer believes that some such expedient is highly desirable in working with very fine colloidal particles of low atomic weight, for in this case the radiation from the air alone far exceeds the ring intensity, and the over-lapping of countless wave-lengths renders a high degree of accuracy improbable.

EXPERIMENTAL

Apparatus

For the investigation of the colloidal nature of beef the writer was fortunate in having at his disposal a well chosen assembly of X-ray diffraction equipment. This equipment consisted of:

(1) The X-ray tube, Muller Metalix, copper target.

(2) Especially designed table with tube and camera mountings.

(3) A selection of cassettes (cameras or film holders) of various types and purposes.

(4) An oscillating crystal spectrograph.

(5) The high tension Power and Control unit.

High Tension Equipment. The high tension power and control unit was of Kelley-Koett design, Type AA. This unit contains an oil cooled sixty cycle transformer with a maximum rating of 2 K.V.A. at 60 K.V. Completely surrounding this high potential source is a cylindrical metal cage, surmounted by a steel table top which is equipped with camera and tube mountings. All high tension leads are enclosed within this protective cage, including the leads to the high potential side of the tube. The voltage produced by the transformer, as well as the filament current to the tube, is adjusted at the remote control panel. The panel is equipped with an adjustable circuit breaker, a minimum water pressure cut-off, voltage regulators and meters, filament rheostat, and the tube milliammeter.

X-Ray Tube. A Muller Metalix X-ray tube adapted for diffraction work was used as the generator of the rays. This tube is of the hot filament, water cooled type, and is equipped with a copper anti-cathode. The tube is completely enclosed in a metal and fibre shell, and carries four small glass windows in its central circumference through which the X-rays leave the tube. The tube is so mounted on the table as to bring these four windows in line

with the four slit or pinhole assemblies which are also mounted on the table. Originally the high tension current was rectified by means of a hot-filament electronic valve. This auxiliary rectifier failed mechanically under the influence of the heat generated in operation, and was replaced by a heavy copper wire. No discernible effect in the operation of the tube was noted after this change, and all further work was done using the unrectified current directly on the X-ray tube.

Photographic Equipment. The photographic equipment consists of the following:

(1) A set of four flat cassettes designed to set firmly on the camera mountings, and to hold the film normal to the X-ray beam. The face of these cassettes was covered with light-proof black paper to protect the films from all but X-radiation.

(2) Two semi-circular cassettes, not used in this work.

(3) Circular cassette made of brass and equipped with a lead lined pinhole opening. This camera with slight remodeling was converted into the vacuum camera previously mentioned.

(4) A Bragg type crystal spectrograph.

(5) Developer, fixer and washing tanks, film holders, solutions and X-ray films.

Experimental Difficulties

Much could be written concerning the multitude of mistakes made in the early part of this work due to a limited knowledge of the properties, and the lack of practical experience with the X-rays. A large share of the first three months labors must be debited to the development of a certain degree of radiographic technique. A mere statement of a few of the difficulties encountered in the quest for reliable quantitative photographs, and their solutions, must here suffice.

(1) Every precaution should be taken to avoid bringing any part of the operators body in the path of the direct rays. Thirty seconds of such experience resulted in deep burns and permanent scar tissue for the writer.

(2) Every material object which receives radiation from the tube, direct or indirect, becomes a secondary source of radiation. This fact is of extreme importance in the case of quantitative diffraction work with a weakly radiating material (such as organic substances) where secondary radiation even from the air has a very appreciable effect. Complete lead housings about the cameras were constructed before a single useful picture was taken.

(3) The time required to expose a film properly, the volt-

age and milliamperage used, must be determined by trial. Often a less intense picture will show more detail and in particular will show the true relative intensities of various parts better than a darker photograph. Time used in practice varies from a few minutes to thirty or more hours.
(4) The selection of filters may be of importance. Papers saturated with nickel salts gave good absorption until the heatof the absorption burned holes through them. Nickel foil was found to be nearly ideal in the case of the copper target tube to filter out all but the K_α line of copper.
(5) The covering over the films in the cassettes for the purpose of excluding visible light and passing X-rays may play an important part in producing good patterns. The original aluminum foil coverings were found to absorb most of the diffracted rays. Two thicknesses of black paper were substituted for the foil coverings, and diffraction patterns could be obtained. Mottling effects on the developed films proved to be due to glue between the two papers. One thickness of black paper was then substituted with good results.
(6) Very little trouble was experienced with the developer and "hypo" solutions. These solutions remained good for several months (water being added occasionally), and were still good when discarded. All photographic work must be

done in intense darkness.

(7) Since three or four photographs are taken at one time, a system must be developed to avoid "switching" the films. This was accomplished by having identifying marks on each cassette which would automatically record on the film.

(8) Adjustment of the pinhole assemblies to pass a sharp and intense pencil of radiation resolves itself into an ordeal of trial and error, using a fluorescent screen to guide the manipulations. Removal of one or both pinhole "plugs" will sometimes materially aid in a preliminary adjustment.

(9) Avoiding the effect of direct radiation striking the film, with the resulting intense black central parts, is accomplished by fixing a small lead cup on the film holder in such a position as to catch the direct beam. By placing a small piece of the fluorescent screen in this lead cup a very convenient visual check of the pinhole alignment is obtained. The foregoing system necessitates using the same camera consistently at one pinhole.

Methods of Studying Meats

Preparation of Samples and Taking of Photographs.

Bearing in mind the facts pointed out in the past several paragraphs, which refer to diffraction work in general, somewhat more should be said of the methods used in study-

ing meat. Attempts were made to get Debye-Scherrer rings from fresh undried meat, but all efforts in that direction proved fruitless. Samples of meat were then dried at 95° Centigrade in a vacuum oven, and were found to give good rings. It was believed that the heat there used would very probably destroy the original structure of the meat by coagulating the proteins. Therefore that method was discarded in favor of a much better one; that of drying the meat cold over concentrated sulfuric acid in a vacuum desiccator. This method proved to be quite rapid, complete, and to give a product with good keeping qualities.

In taking the photographs, a thin slice of the dried sample (0.5 mm. thick) was placed over the outer pinhole (0.04 cm. diameter) and held in place with a little wax which was carefully kept out of the path of the ray. The film holder was then adjusted at five centimeters distance from the pinhole, and normal to the direct ray. The tube was operated at about eighteen milliamperes and at thirty kilovolts for a time varying from two to four hours in most cases. Between the lead discs of the pinhole system was placed a thin sheet of rolled nickel. The nickel foil very effectively removed all intense lines from the X-ray spectrum except the K_α line, which was but slightly affected and which was to be used in the measurements (See Plate XI).

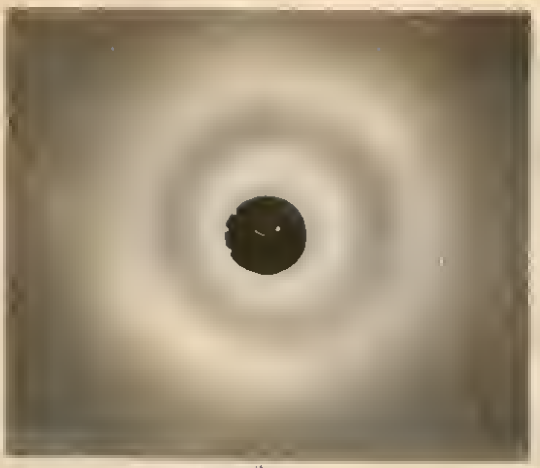

Beef #149

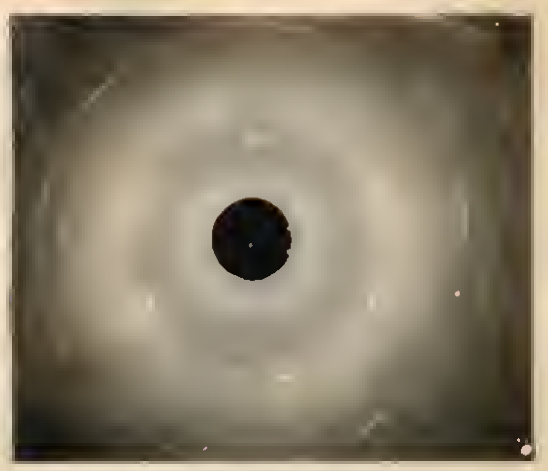

Dried Beef Extract

Cotton-Seed Meal

Navy Bean

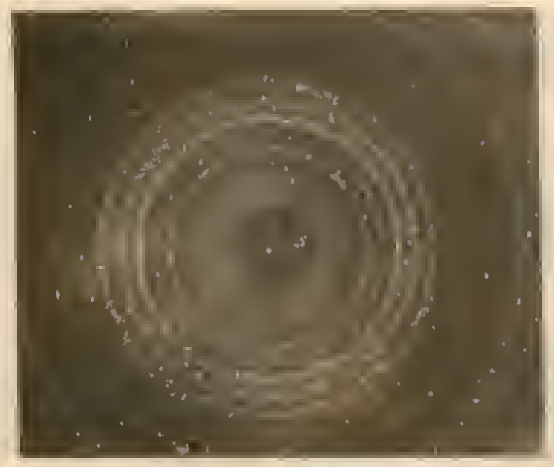

Mannit Powder

Elastic Wax

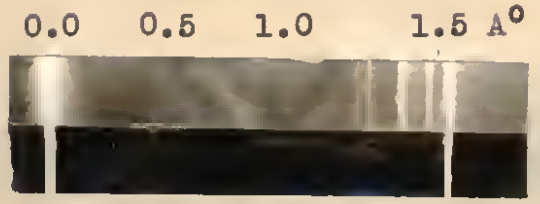

Unfiltered Radiation

Nickel-filtered Radiation

Good ring patterns were obtained from the meats by following this prooedure.

Measurement with Micro-photometer. After a good clear photograph was made it became necessary to convey the information there contained to a graph or curve that it might be studied. The desired graph was one which would show the intensity of darkening of the film at each point along some chosen radius of the ring, and thus make possible the measurement of the half-breadth of the ring (Fig.3).

To serve this function a micro-photometer was built. As the name implies, the micro-photometer is an instrument designed to measure the light transmitted through each point along a line on the film, and thus give a graphic cross-section of the optical density. After several futile attempts to use a polarizing photometer in conjunction with a micrometer-microscope carriage, and later efforts to construct sensitive photo-electric elements for the same purpose, a very satisfactory instrument was evolved similar to that shown by Clark (5).

The micro-photometer in its final form is shown in Figure 2. A twenty-one candle power automobile head-light bulb operating on a constantly controlled current from Edison cells furnished the non-varying light source. The light after being limited by a small circular aperture,

passes through a lens system and is brought to a sharp focus about one inch in front of the photo-electric cell (Weston Photronic Cell, Model 594). Immediately in front of the Weston cell is rigidly fixed a micrometer microscope carriage fitted with a film holder which is so adjusted that the light comes to a sharp focus as it passes through the film. The transmitted light falls on the cell and is transformed into electric current which actuates a very sensitive galvanometer.

The Weston cell when used with the proper external circuit has a straight line relation between current generated and the incident light intensity. It is hence ideal for direct quantitative measurement. The reflecting galvanometer was placed eight feet from the scale, making an effective pointer length of about sixteen feet. The galvanometer used was a Leeds and Northrup instrument (Cat. No 7552) with a rated sensitivity of 2.5 mm. per microvolt and with an internal resistance of 12.6 ohms. It was estimated that one five-hundred thousandths of full sun light would give a deflection of one scale division.

Before measuring the Debye-Scherrer pattern, the center of the ring must be located and marked on the film. This was done by viewing through the film a circle of similar circumference to the Debye ring, the center of which was marked; then by bringing the two circles into juxta-

position, marking on the film the center of the ring. The "centered" film is then placed in the micrometer clips and adjusted to be in the exact focus of the light ray. The micrometer carriage is set to the zero mark and the film moved in the clips to bring the centering mark into the focal point of the light. The micrometer is moved in one-half millimeter increments across the film (along a radius of the ring) and the galvanometer deflections at each setting of the micrometer recorded. It has been found most convenient to record the galvanometer deflections directly on a graph of galvanometer deflection as ordinate versus distance from the center as abscissa. By virtue of the straight line characteristics of the Weston cell, this "galvanometer deflection vs. displacement" curve becomes the "intensity vs. displacement" curve which is desired. It is this curve (Fig. 3) that is considered to be the "original curve" of the meat pattern. It is this curve which must be rectified and measured before the colloidal particle size can be determined.

Air-Scattering Check. As has been suggested prior to this point, a blank or air-scattering pattern was made. In taking this photograph methods identical to those used in taking a normal meat pattern were followed. The resultant photograph when converted to the graphical form by the

micro-photometer, and plotted to the same absolute scale (obtained by setting galvanometer needle to zero where the film was unexposed, i.e. under the lead cup) as was the theoretical air-scattering curve ($I_x = \frac{1}{x} - \frac{1}{\sqrt{x^2 + 24.5}}$) was found to agree almost perfectly (Fig. 9). To make certain the air and not the dust particles in the air were giving this curve, a run was made using dried and filtered air in a closed camera. The result was in every way comparable with the former curve. The results of these measurements were taken as a direct vindication of the methods and technique used throughout the work.

Scattering Factor of Meat. The "scattering-factors" used in the calculations were determined by measuring the intensity of the rays scattered by a thin slice of the dried meat at all angles to the primary beam. The necessary photograph was taken on a film wrapped around the inner wall of a cylindrical metal camera. The X-radiation entered along a radius of the cross section, struck the thin sample of meat at the center, and left the camera through an opening diametrically opposite the entering point without making contact with any other matter. The camera was attached to a vacuum pump and the pressure held at about two-tenths centimeter of mercury for the duration of the run to avoid the effect of air-scattered radiation.

The film (after developing) was studied by means of the micro-photometer, and the intensity plotted against the angle to the primary ray. The intensity relations were also plotted in polar coordinates, and the "scattering factor" determined. The "scattering factor" is the ratio of the intensity at any angle (or corresponding displacement on the film) to the intensity of the radiation parallel to and in the direction of the primary ray. Figure 4 shows graphically this distribution of the scattered radiation. The curve here obtained compares closely with that shown by Crowther (7) for aluminum foil. It varies from the form derived by the Electro-magnetic theory, $I_\theta = I\frac{\pi}{2}\left(1+\cos^2\theta\right)$, in that it is not symmetrical, being much more intense in the direction of the primary beam.

Characteristics of Radiation Used and Stripping Curves. All spectrum analysis of the primary X-radiation was done on a Bragg type oscillating crystal spectrograph, manufactured by the J.B. Hayes company. Extensive shielding was essential to give quantitative measurements of the spectrum obtained. "Base line" deductions also had to be made in the case of the spectrum measurements.

Qualitative study of the spectrum revealed the shortest wave produced, at 0.425 A° (corresponding to 29 K.V.), the silver and bromine absorption edges, and seven bright lines.

Of the seven lines, five were identified as the "L" series of tungsten (splattered from the filament) and the remaining two as the K_β and K_α of copper. In addition to these definite parts was also the general "white" radiation, reaching from the shortest wave length onward. Filtering the X-ray through the nickel foil removed all visible lines but the K_α of the copper, which was but slightly absorbed. Penetrating the nickel in addition to the K_α line was a large proportion of the shortest of the rays and a considerable share of rays longer than the K_α line. Plate XI shows the original unfiltered ray and also the marked effect of the filtration. A photograph of the filtered spectrum was made, taking every precaution to avoid stray radiation. This carefully prepared spectrum was measured quantitatively on the micro-photometer to determine exactly the character of the radiation being used in the next analysis. Figure 5 shows graphically the result of these measurements, as well as the relative energy represented in the one-tenth Angstrom Unit increments.

Making use of the energy distribution data obtained from the above measurements and the reaction which particles of known size would have with each wave length increment (according to the resolving power formula, $D = \frac{K}{d\lambda}$ and the law $n\lambda = 2\,d\,\sin\theta$), the previously mentioned

series of composite curves was built up. By plotting the stripping factors thus obtained corresponding to a certain distance from the center against the assumed particle size, the stripping factor for intermediate sizes may be read from the graph. Repetition of the above procedure for each distance from the center gives the complete "Stripping Curve" graph (Fig. 11). On the same set of coordinates is also plotted the base line factor. This factor is a number by which to multiply the distance "h" (Fig.12) to arrive at the distance "m-n", the difference in intensity between the original curve and its corresponding base line at a point twelve millimeters from the center. It is this point "m" together with the "o" on the original curve at thirty-five millimeters from the center that serves to locate the base line with respect to the original curve. This base-line factor is obtained from the same set of curves as is used to build up the series of stripping factors.

Measurement of the Particle Size

To unify the many steps in the particle size measurement and to illustrate the process here used, the following resume' is given:

(1) Obtain Debye-Scherrer patterns of the dried meat sample.

(2) Convey the Debye-Scherrer pattern to a graphical form by the use of the micro-photometer.

(3) Connect the point on the curve twelve millimeters from the center to the point thirty-five millimeters from center. Draw a line connecting the apex of the ring (17 mm. for the most) to the 12-35 mm. line at seventeen millimeters from the center. Measure this distance "h" (Fig. 12).

(4) From the general shape and slope of the original curve, assume a particular particle size.

(5) Find on stripping chart the factor by which to multiply the "h" to give distance of base line below the original curve at 12 mm. from the center.

(6) Reduce the base line (Fig. 8) to such a scale that it will pass through points "o" and "n". Sketch the base line through these points.

(7) Plot difference of ordinates between original curve and base line against the distance from center, on same paper as the original.

(8) Multiply the ordinates at each integral millimeter distance from the center by the proper stripping factor, corresponding to the assumed particle size, and plot the new curve.

(9) Measure the width of the ring at one-half maximum intensity and apply in the formula $\delta = \frac{K}{d\lambda}$, obtaining the $d\lambda$

from the " λ—distance from center" graph (Fig. 13).
(10) If the calculated "D" agrees closely with the assumed particle size, the assumption was correct. If the calculated diameter varies appreciably from the assumed, repeat the process beginning with step four of this outline. Repeat until the assumed particle size checks closely (within about 0.3 A° throughout this work) with the measured value.

Two corrections have not been made by this process. The diameter of the pinhole and the varying distance of the ring parts from the pinhole have been neglected. It is believed that these two factors, working in opposition, will partly compensate for each other, and also, since they are constant throughout all measurements, will not alter the order of magnitude of the particles.

The possibility existed that the particle size thus determined might be that of small inorganic crystals of water soluble salts. The space-lattice of the particles was found to be 4.73 A° as compared with 2.814 A° of sodium chloride, hence this possibility seems unlikely. However, a sample of ground meat was thoroughly leached with water to remove all soluble matter, and the dried wash liquors as well as the insoluble portions subjected to X-ray study. The portion which was free of soluble salts gave the normal meat pattern, while the dried aqueous

fraction gave a pattern resembling that of a fibre. The result quite definitely fixed the particle size being measured with the bulk of the meat and not with a chance formation of various salt crystals.

It might be here noted that early tests were run on various meats including frog, insect, fish, pork, mutton, beef and human skin. All of these revealed the same space lattice distance (d in the formula, $n\lambda = 2d \sin\theta$), within experimental error. This rather unexpected finding makes possible the use of the curves here developed and the same resolving power constant ($K = \frac{\lambda^2}{2\sin\theta} = 7.53$) to measure the particles of the various meats.

The meats studied in this work were of twelve head of Hereford cattle raised by the Animal Husbandry Department. These animals were divided into several lots and fed differently, the objective of the project being to determine the relative advantages of several feeding methods for beef cattle. Suffice it here to state:

Lot Number 1.

Animals 131, 125, 147, and 142. Full feed of grain and cotton seed with alfalfa hay, in dry lot.

Lot Number 2.

Animals 144, 135, and 134. Full feed of grain and cotton seed, on pasture.

Lot Number 3.

Animals 126 and 149. Pasture only.

Lot Number 4.

Animals 28 and 29. Holstein bulls fed on milk only, in stalls.

Lot Number 5.

Animal- Armour Dark Cutter.

Chemical and Physical data other than particle size determinations on these meat samples were obtained from Dr. J. L. Hall and Mr. H. W. Loy of the Chemistry department, both of whom have worked on the beef project.

Results

Table 1 shows several of the particle size determinations as calculated by the Debye-Scherrer, the Bragg, and the Resolving Power formulae. The particle sizes shown were calculated by the respective formulae using the same ring breadth in each case, and neglecting the pinhole corrections. It will be seen that the values given by the Resolving Power formula are greater than the Debye-Scherrer values by about the same amount as the Bragg values are lower. All formulae are in fair agreement.

Table 1. Comparison of Particle Size Equations

Meat	Bragg	Debye-Scherrer	Resolving Power	Average
#121	16.9A°	17.8A°	19.0A°	17.9A°
#135	14.3	15.1	16.0	15.1
#149	11.4	12.1	12.8	12.1

Table 2 brings together all of the data collected on the various meat samples, in decending order of particle size. Of the various sets of data no correlations were found except an apparent periodic relation between the particle size and Surface Distribution of Shrinkage (Evaporation per unit surface area during storage). This correlation is best seen in graphical form (Fig.14). It will further be noted that animals of the same feed lot tend to have the same size meat particles. In this regard it will be seen that Feed and Pasture animals (Lot 2) 144, 135, and 134 are together in the particle size series. Also the milk fed bulls, #28 and #29 are together in the series when fresh and continue to be together after ripening. Ripening, in the case of the bulls #28 and #29 resulted in a growth of particle size. A fresh sample of the Armour Dark Cutter gave a very sharp ring pattern, indicating large particle size. The micro-photometric curve could not

Table 2.

Heat Number	Lot Number	Particle Size	Surface Distribution of Shrinkage	Turbidity Factor	Electrical Resistance	Ca-Ca Ratio
121	No.1.	19.0	405	0.69	158	10.25
125	No.1.	18.2	389	1.06	182	4.63
28-R	No.4.	17.1	---	---	---	---
29-R	No.4.	16.8	---	---	---	---
144	No.2.	16.7	462	0.40	123	2.89
135	No.2.	16.0	438	1.23	183	6.79
Arm.	No.5.	15.9	422	1.29	365	3.74
134	No.2.	15.8	398	0.32	203	5.84
126	No.3.	15.2	438	1.46	216	5.21
28-F	No.4.	15.2	556	0.39	358	4.80
29-F	No.4.	14.7	484	0.60	215	5.67
147	No.1.	13.4	405	0.63	180	8.66
148	No.1.	13.1	465	0.70	189	6.36
149	No.3.	12.8	590	1.01	329	3.91

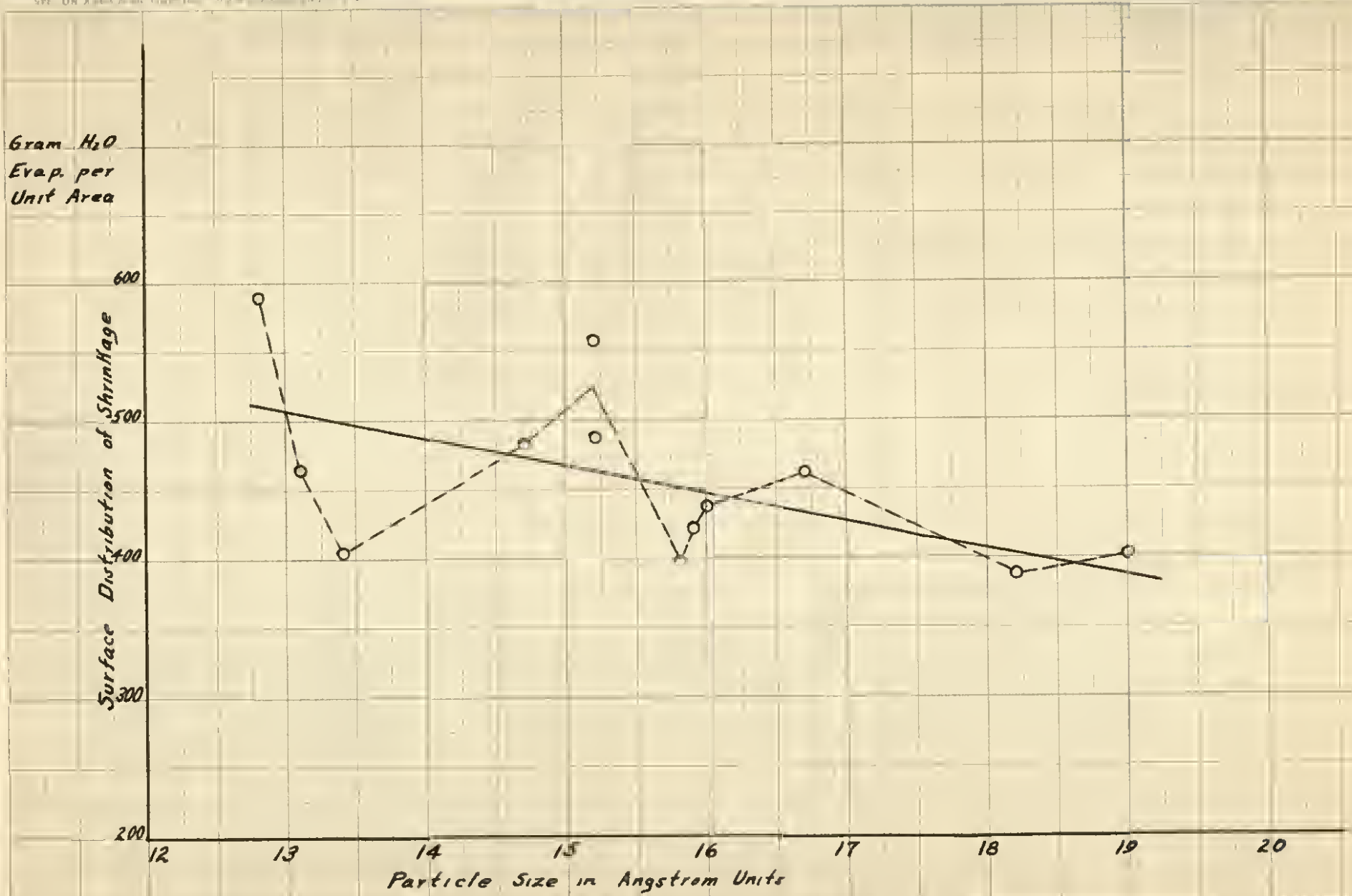

Fig.14. Showing Relation of Surface Distribution to Particle Size

be measured for particle size due to its very peculiar shape. The ripened sample, however, returned to a normal form and appears from particle measurement to be an average beef.

Conclusions

Beef, and other meats, when properly dried possess a sufficiently regular atomic or molecular arrangement to give definite diffraction effects. The distance over which this regular marshalling of points extends is well within the colloidal range, and quite probably represents a single protein molecule. Assuming a cubic shape of the particle and calculating from the density of the dried meat, each particle contains from 140 to 500 carbon atoms or the weight equivalent. This, if the particles are in reality molecules, gives the meat particles a molecular weight of from 1500 to 6000, somewhat lower than usually estimated for a complex protein. This difference may be due to the fact that the pinhole correction was not applied, or to an actual breaking of the molecule in drying.

From ring radius measurement it is calculated for all the meats studied that the diffracting planes are 4.73 Angstrom Units apart. Hence, in the case of a 20 A^{0} particle, there are about four parallel planes producing the diffraction. Again assuming the cubic arrangement, the

atomic groups probably lie on four parallel planes in each of the three dimensions, making a total of 64 point groups. Dividing the 64 point groups into the corresponding molecular weight, 6000 (for the 20 A^0 particle), indicates each point group has a molecular weight near 100, corresponding roughly to an average amino acid.

There seems to be a difference in the size of the colloidal particles in various samples of beef which is measurable by X-ray diffraction methods. This work indicates that the size of the colloidal particles is some function of the feeding methods; this is not, however, conclusive, as it is based upon an insufficient number of samples for generalization.

Particle size could not be correlated with electrical resistance, turbidity of the aqueous extract, nor the sodium-calcium ratio. A somewhat periodic relation between evaporation from the surface (Surface Distribution of Shrinkage) and particle size appears to exist. Although the relation is subject to extreme fluctuations of a periodic nature, a general trend toward lower shrinkage losses with increased particle size seems to be evident.

SUMMARY

The technique necessary to produce good Debye-Scherrer

patterns from beef was developed, and the patterns were obtained from the meats to be studied. These patterns were converted by means of the micro-photometer to a graphical form for measurement. By first discounting the effects due to the amorphous scattering from the meat and the air, and then by removing the effect of all but the K_α radiation of copper, the unmodified Debye-Scherrer ring was obtained for measurement. Measurement of the Half-breadth of this ring together with a knowledge of the wave length being used and the mean ring radius, made possible the calculations of the particle size of the beef. Study of the particle size measurements in connection with the history and other characteristics of the meat indicated a relation between:

(1) Particle size and feeding method.

(2) Particle size and the ripening process.

(3) Particle size and the shrinkage loss.

ACKNOWLEDGMENTS

The writer desires to express his appreciation to Dr. H. H. King, his major instructor, for making this investigation possible: and to Dr. J. Lowe Hall for suggesting the problem and under whose guidance the work was pursued. The writer further extends his thanks to the other members of the Chemistry and Physics Departments who materially aided him in his work.

BIBLIOGRAPHY

(1) Baly, E.C.C.
Spectroscopy. London.
Longmans, Green & Co. 653 p. 1912.

(2) Bragg, W.H. and Bragg, W.L.
X-rays and crystal structure. 2 ed. London.
G. Bell and Sons. 325 p. 1915.

(3) Clark, George L.
Applied X-rays. New York.
McGraw Hill. 243 p. 1926.

(4) ----
X-rays as a research tool in chemistry and industry. Industrial and Engineering Chemistry.
24:182-190. Feb. 1932.

(5) ----
X-ray metallography in 1929.
Metals and Alloys. July to Nov. 1929.

(6) Coven, Allen W.
Scattering of X-rays from paraffin at angles.
The Physical Review. 38:1424-31. Oct. 15, 1931.

(7) Crowther, James Arnold.
Ions, electrons, and ionising radiations. 4 ed.
London. Edward Arnold & Co. 323 p. 1919

(8) Meyer, Alfred Merley.
Diffraction of X-rays in organic mixtures.
The Physical Review. 38:1083-93. Sept. 15, 1931.

(9) Siegbahn, Manne. ed. by Lindsay, George A.
The spectroscopy of X-rays. London.
Oxford University Press. 246 p. 1923.

(10) Terrill, H.M. and Ulrey, C.T.
X-ray technology. New York.
D.Van Nostrand Co. 250 p. 1930

(11) Wyckoff, Ralph W.G. ed. by Noyes, William A.
The structure of crystals. 2 ed. New York.
The Chemical Catalog Co. 393 p. 1931.